arXiv:1604.05515v1 [cond-mat.mtrl-sci] 19 Apr 2016

Ab initio Study of Aspirin Adsorption on Single-walled Carbon and Carbon Nitride Nanotubes

Yongju Lee,[1] Dae-Gyeon Kwon,[1,*] Gunn Kim,[2,†] and Young-Kyun Kwon[1,‡]

[1] *Department of Physics and Research Institute for Basic Sciences, Kyung Hee University, Seoul, 02447, Korea*

[2] *Department of Physics & Astronomy and Graphene Research Institute, Sejong University, Seoul, Korea, 05006, Korea*

(Dated: April 20, 2016)

Abstract

We use *ab intio* density functional theory to investigate the adsorption properties of acetylsalicylic acid or aspirin on a $(10, 0)$ carbon nanotube (CNT) and a $(8, 0)$ triazine-based graphitic carbon nitride nanotube (CNNT). It is found that an aspirin molecule binds stronger to the CNNT with its adsorption energy of 0.67 eV than to the CNT with 0.51 eV. The stronger adsorption energy on the CNNT is ascribed to the high reactivity of its N atoms with high electron affinity. The CNNT exhibits local electric dipole moments, which cause strong charge redistribution in the aspirin molecule adsorbed on the CNNT than on the CNT. We also explore the influence of an external electric field on the adsorption properties of aspirin on these nanotubes by examining the modifications in their electronic band structures, partial densities of states, and charge distributions. It is found that an electric field applied along a particular direction induces aspirin molecular states in the in-gap region of the CNNT implying a potential application of aspirin detection.

I. INTRODUCTION

Acetylsalicylic acid (ASA), also known as aspirin, has been one of the most widely used medications in the world due to its well-known effects of reducing fevers and relieving aches and pains. Aspirin has been used to help prevent heart attacks, strokes, blood clot formation and suppression of prostaglandin owing to its antiplatelet effect of decreasing platelet aggregation and inhibiting thrombus formation.[1] It has also been reported that aspirin has an anticancer effect[2] and a precautionary effect on stroke[3]. Despite of such good effects, however, it has been warned that such a famous non-prescription medicine may provoke some adverse effects and thus people should avoid its substance (drug) abuse and misuse. Because aspirin has an effect on the stomach lining, it is recommended that people with gastroenteric disorders such as gastritis and peptic ulcers take medical advice before using aspirin. When aspirin is taken with alcohol, stomach bleeding may occur even to healthy people. Therefore, it is important to measure the amount of ASA molecule in solution or in human body.

Carbon nanotubes (CNTs) are thin and long macromolecules of graphitic carbon that have attracted huge academic and industrial interest because of unique physical and chemical properties[4–14]. One of the attractive characteristics of the CNT is a very large adsorption surface area[15–17] comparable to that of carbon-based adsorbents (such as activated carbon) used commercially. Several binding properties of molecules onto the CNT have been also studied theoretically and experimentally[15,18–23] for its applications. Using the property of the large adsorption surface areas, CNT can be used to filter or to detect molecules. Since some gas molecules such as ammonia (NH_3)[24], nitrogen dioxide (NO_2)[24], alcohol[25], and other molecules[26–29] were reported to be detectable by these devices, a wide range of molecules have been studied for chemical sensing of CNT. Due to the modification of intrinsic electronic structures of semiconducting CNT by adsorption, the type and concentration of target molecules may be detected.

Carbon nitride compounds have been studied in various area such as electronic devices, humidity sensor, and coatings because of their electronic and chemical properties[30–32]. They have various structures, depending on their carbon to nitrogen atomic ratio and arrangement. In this study, we focus on a graphitic carbon nitride (g-C_3N_4) nanotube (CNNT), triazine-based form. Recent studies report g-C_3N_4 nanotube with respect to synthesis and first-

principles calculations[33–36]. Various adsorption properties are expected because of the unique porous structure.

In this paper, we present a first-principles study of binding properties of ASA on the bare CNT and the bare CNNT. ASA binds to pristine CNT (CNNT) with binding energy of 0.51 eV (0.67 eV), and no practical charge transfer takes place. According to our analysis on the electronic structure, CNT with ASA adsorbates does not show significant characteristics, but CNNT with ASA adsorbates show noticeable effects. Because of the structure of the CNNT, local electric dipole moments occur and interrupt exchange of electrons between the ASA molecule and the CNNT. Finally we discuss homogeneous external electric field (E-field) effects on the CNNT with ASA adsorbates. The response of nanotubes to the E-field is attractive for the application to electric devices.

II. COMPUTATIONAL METHOD

Using the first-principles calculations based on density functional theory (DFT)[37,38], we examined the CNT and the CNNT with respect to the adsorption of ASA. The electronic wavefunctions were expanded into plane waves up to a cutoff energy of 450 eV, and the ion-electron interactions were described using the projector augmented wave method implemented in the Vienna *ab initio* simulation package (VASP)[39,40], within the generalized gradient approximation (GGA) method[41]. To better describe interaction between ASA and nanotubes, we considered van der Waals interaction using Grimme's method (DFT-D2)[42]. All the model structures were relaxed until the Hellmann–Feynman forces were smaller than 0.03 eV/Å. We chose the $(10, 0)$ CNT and the $(8, 0)$ CNNT as host materials for molecular adsorption. For the calculation of the ASA molecule in vacuum, we used a cubic supercell with a length of 30 Å. The Γ-point were used in calculations of the isolated ASA molecule. The lengths of the supercell along the tube axis were 16.05 Å for the CNT, and 15.72 Å for the CNNT, respectively. We used one k point (the Γ-point) for the nanotubes in the geometry optimization, and $1 \times 1 \times 10$ Monkhorst- Pack[43] k point sampling in the electronic structure calculations. For each adsorption configuration, we calculated binding energy (E_b) defined by Eq. 1. E[tube+ASA] is the total energy of the CNT and the CNNT with an ASA molecule, and E[tube] is the total energy of the two nanotubes without any ASA molecule, respectively. E[ASA] also shows the energy of the isolated ASA molecule.

$$E_b = E[\text{tube}] + E[\text{ASA}] - E[\text{tube} + \text{ASA}] \quad (1)$$

III. RESULTS AND DISCUSSION

Fig. 1(a) shows the most stable structure of an ASA molecule ($C_9H_8O_4$) in vacuum. It consists of an aromatic ring, ester, and carboxylic acid. Fig. 1(b) and (c) show the highest occupied molecular orbital (HOMO) and the lowest unoccupied molecular orbital (LUMO), respectively. Its HOMO–LUMO gap is 3.75 eV. In the HOMO and the LUMO of ASA, electronic densities are distributed over the entire molecule, as shown in Fig. 1(b). We selected the two types of nanotubes to investigate their application for detecting ASA molecules: the $(10, 0)$ CNT and the $(8, 0)$ g-C_3N_4 nanotube. As shown in Fig. 2(a) and (b), the bare $(10, 0)$ CNT has a band gap of 0.88 eV, and the bare $(8, 0)$ CNNT has a band gap of 2.55 eV.

When an ASA molecule is adsorbed on nanotubes, many possible configurations can be considered. We chose only $\pi - \pi$ stacking configurations, and calculated the total energy of each configuration to obtain the most stable adsorption site. For visual clarity, the carbon atoms of the ASA molecule is shown in yellow, while those of the CNT and the CNNT is represented in black (Fig. 2). For the binding of ASA on the $(10, 0)$ CNT, the most stable configuration resembles Bernal stacking (AB stacking) of graphite, as seen in Fig. 2(a). Its electronic band structure shows no clear change near the Fermi level compared with that of the bare CNT, even if flat bands originating from the ASA molecule are shown around -2 eV and $+2$ eV. Fig. 2(b) shows the most stable adsorption configuration of the CNNT with ASA adsorbates. Nitrogen atoms located in the benzene ring of ASA and the carboxyl group of ASA is placed just above pore sites of the CNNT. The band gap slightly decreases by 0.07 eV. Since $\pi - \pi$ hybridization is the main origin of the molecular binding, noticeable charge transfer does not occur. Consequently any molecular state from ASA is not shown in the band gap of the CNT or the CNNT. We conclude that it is difficult to detect ASA using the CNT or the CNNT in the absence of external E-field. Table I summaries the adsorption energy and the distance between the ASA molecule and the tube wall for each adsorption configuration. We find that ASA binds more strongly to the CNNT than the CNT.

To understand the difference in the adsorption energy between the CNT and the CNNT,

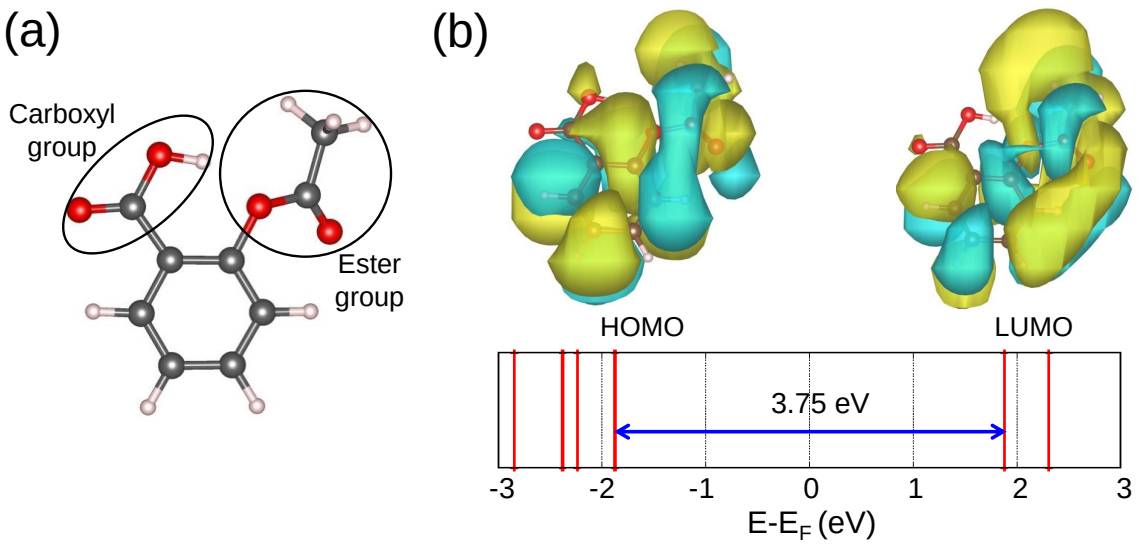

FIG. 1. (a) Model structure of an ASA molecule. (b) Electronic energy levels of an ASA molecule with wavefunctions of its HOMO and LUMO. The HOMO–LUMO gap is 3.75 eV.

we studied the interaction between the ASA molecule and the CNT and CNNT in more detail. Fig. 3(a) and (b) shows a charge difference $[\rho(\text{tube} + \text{ASA}) - \rho(\text{tube}) - \rho(\text{ASA})]$ plot of the $(10, 0)$ CNT and $(8, 0)$ CNNT with ASA, respectively. As mentioned above, there is no charge transfer between the ASA molecule and both nanotubes. Interestingly, we observe that the much bigger charge redistribution appears in the ASA molecule with CNNT than CNT. What makes the charge redistribution in ASA? Because of the electronic configurations of the C and N atoms, the nanotube forms a buckled structure contrary to CNT's structure. Lone pair electrons, which are localized at the N atoms, result in buckling of the tube surface. In addition, we can take into account local electric dipole moments of the CNNT. The difference in the electron affinity of the C and N atoms causes the local electric dipole moments, which are obtained by Eq. 2. Electric dipole moments of the CNNT are shown in Fig. 3(c). As a result, local electric dipole moments together with buckling and vacancies bring about the charge redistribution of ASA.

$$\int \rho(r) r dr + \sum_i Z_i e z_i \tag{2}$$

Fig. 3(c) depicts local electric dipole moments in the surface of the CNNT. Above all, the nitrogen atoms with red arrows are more buckled in a different direction from those with

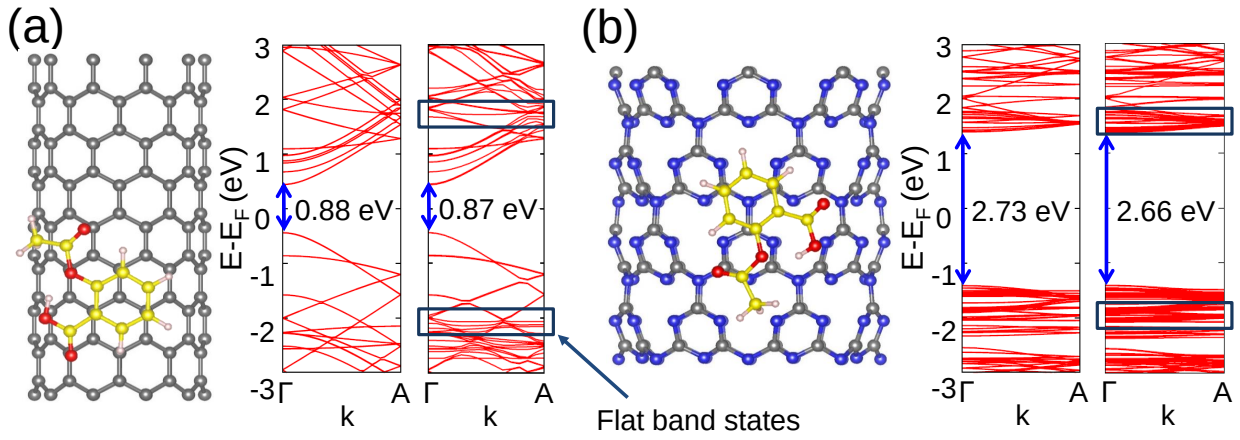

FIG. 2. Electronic property of ASA adsorbed on (a) the CNT and (b) the CNNT. The most stable adsorption sites among possible configurations (left) and band structures of the bare nanotube (middle) and ASA on nanotube (right). The flat bands in the rectangles originate from the ASA molecule on the tube.

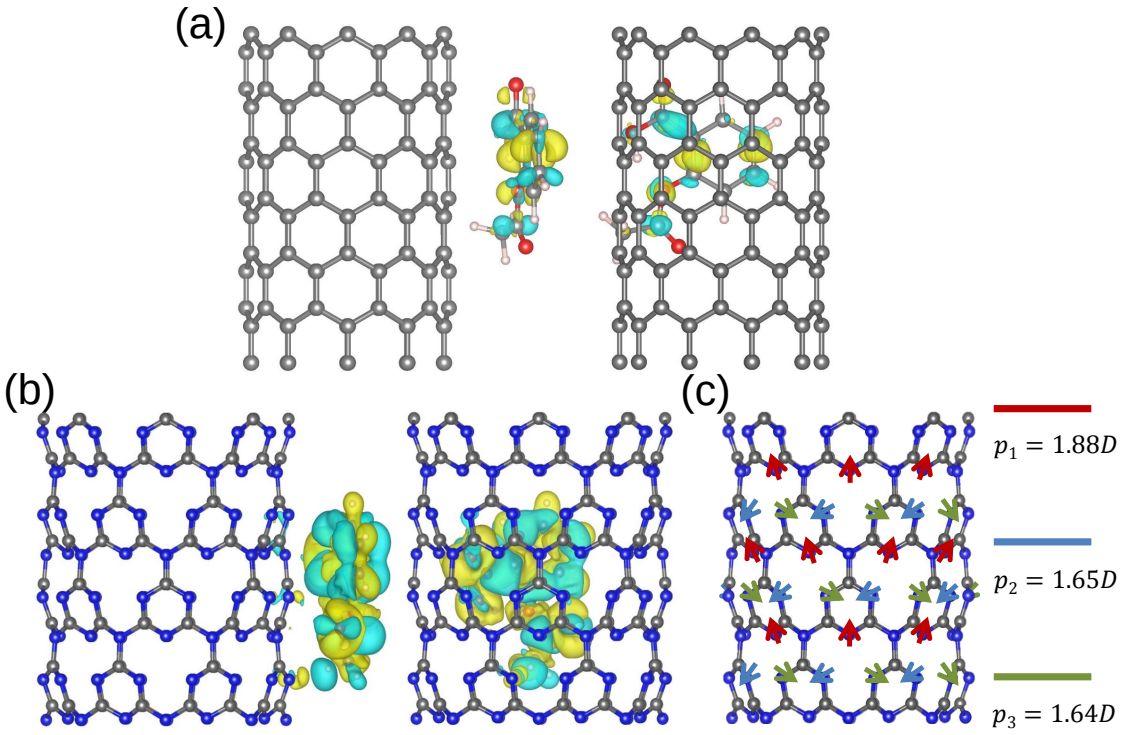

FIG. 3. (a) Charge difference of the ASA-adsorbed CNT and (b) charge difference of the ASA-adsorbed CNNT. (c) Directions and magnitudes of electrical dipole moments in the bare CNNT. Cyan and yellow colors represent electron accumulation and electron depletion, respectively. D is the unit of the electric dipole moment, debye.

green and blue arrows. Therefore, the dipole moments denoted by green and blue arrows have almost similar values, 1.64 D and 1.65 D, respectively. (1 D $\approx 3.336 \times 10^{-30}$ C $\cdot$ m ≈ 0.2082 e$\cdot$Å), respectively, while those by red arrows are bigger (1.88 D). Because of the local electric dipole moments, the ASA molecule has dipole-dipole interaction with the CNNT. ASA in vacuum has an electric dipole moment of 1.51 D, but ASA on the CNNT has a larger moment of 2.25 D. If a simple dipole-dipole interaction (V_{dd} in Eq. 3) is applied with the aforementioned dipole moments at the ASA molecule and the CNNT, the interaction energy is about -0.1 eV. It explains the difference in the binding energy listed in Table I. We conclude that the aspirin molecule adsorbs more strongly on the CNNT than the CNT owing to the dipole-dipole interaction.

$$V_{dd} = \frac{1}{4\pi\epsilon_0}\left[\frac{\vec{p}_1 \cdot \vec{p}_2}{|\vec{r}_1 - \vec{r}_2|^3} - \frac{3\{(\vec{r}_1 - \vec{r}_2)\cdot\vec{p}_1\}\{(\vec{r}_1 - \vec{r}_2)\cdot\vec{p}_2\}}{|\vec{r}_1 - \vec{r}_2|^5}\right], \tag{3}$$

where V_{dd} is a potential energy for dipole-dipole interaction, and $\vec{p}_i$ and $\vec{r}_i$ ($i = 1, 2$) are the i-th electric dipole moment and its position, respectively.

To check whether the nanotube can be applied to a detecting device for ASA molecules, we checked effects of external E-field on electric property of the bare CNNT and ASA-adsorbed CNNT. In a single-gated field effect transistor, an E-field is generated by an applied gate bias between the gate and the nanotube. Our computational results reveal the difference between the electronic structure of the bare CNNT and ASA-adsorbed CNNT. Band gap of the bare CNNT is shown much smaller than ASA-adsorbed CNNT. Not only there are the difference of band gap between the bare CNNT and ASA-adsorbed CNNT, but also the different electronic property among four directions. The electronic structure of the ASA-

TABLE I. The binding energy and the distance between the adsorbed molecule and nanotubes. (C_3N_4 + ASA 2, 3 in Supplementary Information.)

Structure	Binding energy (eV)	Distance (Å)
CNT + ASA	0.54	2.59
C_3N_4 + ASA 1	0.66	2.70
C_3N_4 + ASA 2	0.68	2.68
C_3N_4 + ASA 3	0.67	2.72

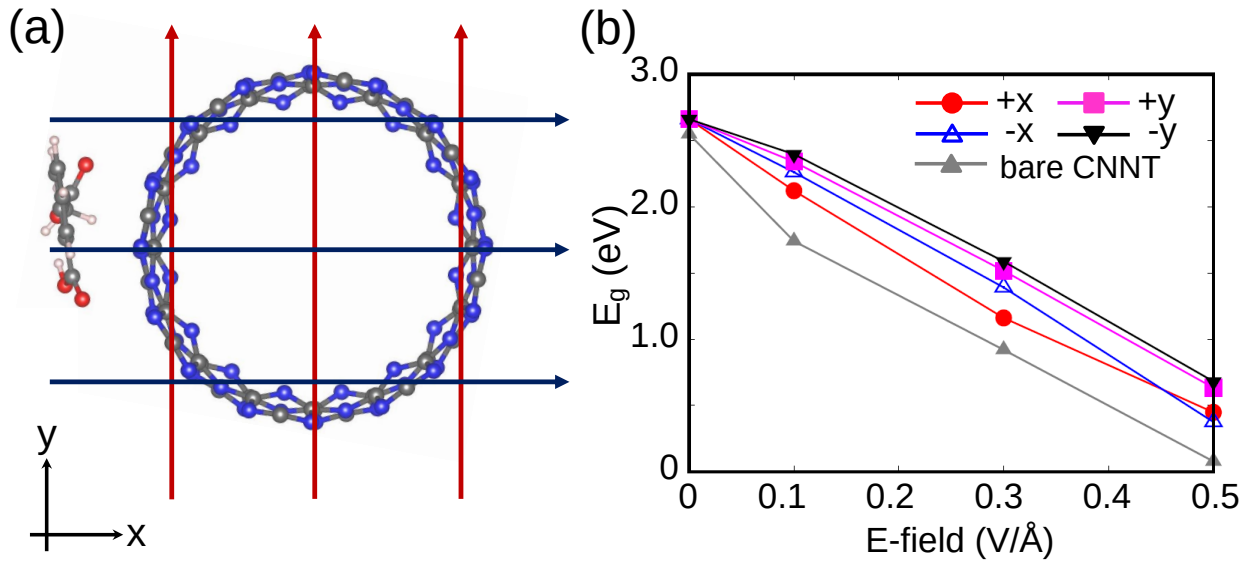

FIG. 4. (a) Directions of external electric field on the ASA-adsorbed CNNT. (b) Band gaps of bare CNNT and ASA-adsorbed CNNT in all directions of the external electric field. The x directions in (a) cross both of the ASA molecule and the CNNT perpendicularly. The y directions also cross CNNT perpendicularly, but ASA molecule horizontally. They tend to decrease according to intensity of electric field.

adsorbed CNNT is not affected very much by the E-field perpendicular to the tube axis. In contrast, the ASA-adsorbed CNNT show remarkable characters in the band structure, depending on the direction of the transverse E-field, as shown Fig. 4. We chose four directions of the E-field ($\pm x$ and $\pm y$), which were all perpendicular to the CNNT axis direction. The E-fields in $\pm x$ directions may enhance electronic coupling between the ASA molecule and the CNNT, whereas the fields in the $\pm y$ directions show the weak ASA-CNNT coupling. Fig. 4(b) shows that the external E-field can modulate the electronic structure of the ASA-adsorbed CNNT. We also present partial densities of states (PDOS) of the ASA-adsorbed CNNT in Fig. 5. Since the E-field is in the $+x$ direction and the CNNT has a higher electric potential than the ASA adsorbate, electrons are donated from adsorbed ASA molecule to one part of the CNNT. Fig. 5(a) shows that the transverse E-field in the $+x$ direction makes localized states of the ASA molecule be upshifted, and move into the + region of the CNNT, as the E-field strength increases. Besides the conduction band of the tube also moves down to the Fermi level. On the other hand, the E-fields in $-x$, $+y$ and $-y$ directions have the similar tendency; Although the band gap decreases, the states originating from ASA do not

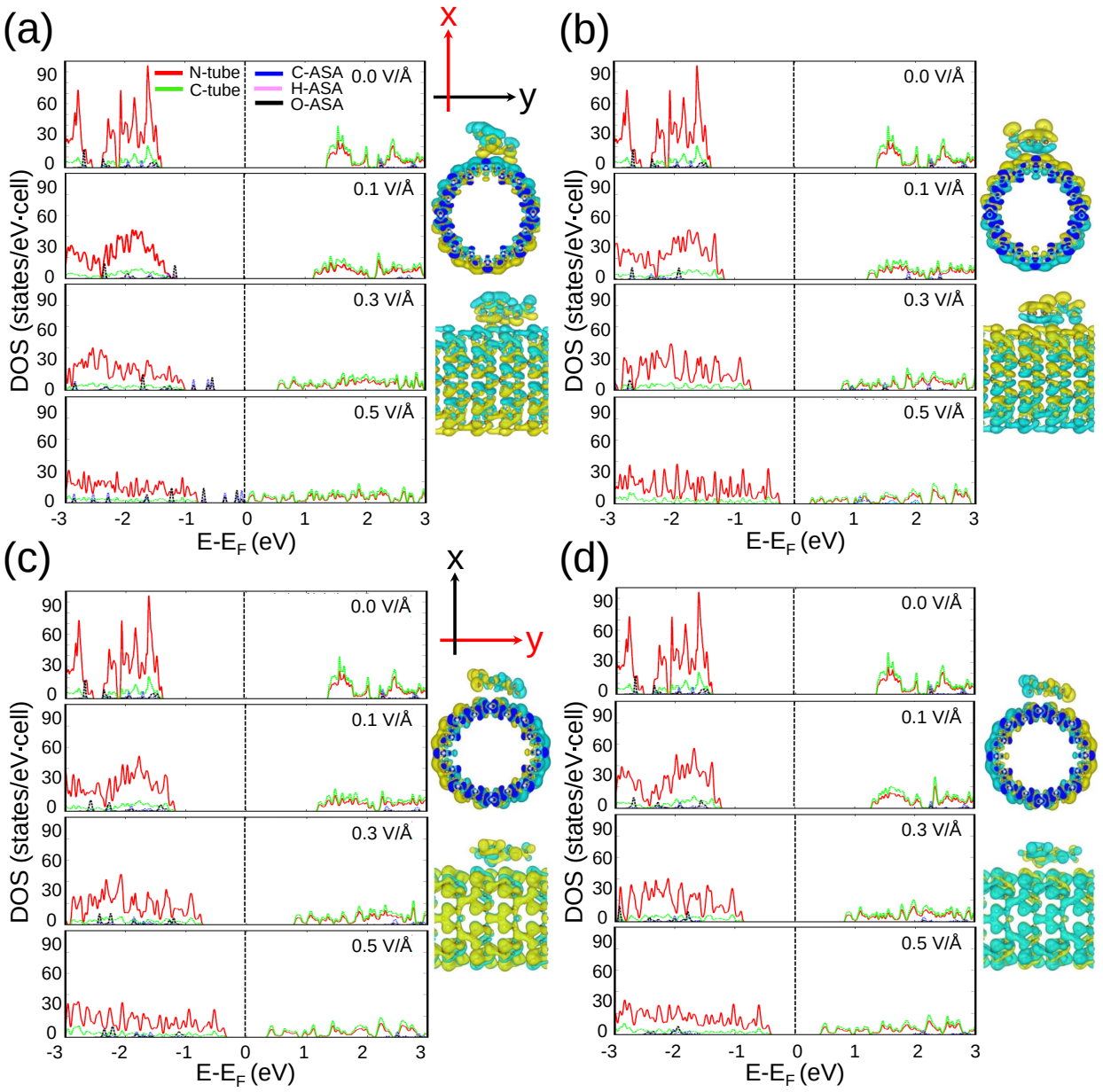

FIG. 5. (a-d) PDOS plots and electron density differences of the ASA-adsorbed CNNT under the external E-fields in $\pm x$ and $\pm y$ directions, respectively. The arrow means the direction of E-field. Charge transfer occurs due to the external E-field. Cyan and yellow colors represent electron accumulation and electron depletion, respectively.

appear as the in-gap states. In both $\pm y$ directions, external E-field does not cause strong ASA-CNNT coupling enhancement, which is related to the reflection symmetry. The band gap of the bare CNNT is also reduced under external E-field, but there is no localized states in the energy band gap in this case. In real situations, the CNNT would be coated with ASA

molecules randomly, and thus any direction of the E-field makes the ASA states occur in the forbidden band. Such in-gap states could result in the scattering in the electron transport, which would be reflected in the current-voltage curve in experiment. Consequently, the C_3N_4 nanotube-based sensor device may detect the ASA molecules using the gate bias voltage (or external E-field).

IV. CONCLUSION

In summary, we have performed *ab initio* calculations within density CNNT. ASA is adsorbed more weakly on the CNT than the CNNT. Since CNNT have local electric dipole moments, it causes a stronger binding to ASA than the CNT owing to dipole-dipole interaction of the CNNT with the ASA molecule. When a homogeneous external electric field is introduced, the band gap of the CNNT decreases dramatically in the presence of the ASA adsorbates. Especially, when $+x$ direction is applied, in-gap states of aspirin molecule occur. Thus we expect that CNNT could be used in application to chemical sensors based on the field effect transistor.

ACKNOWLEDGMENTS

We gratefully acknowledge financial support from the Korean government through National Research Foundation (NRF-2011-0016188). GK were supported by the Priority Research Center Program (2010-0020207) and the Basic Science Research Program (2013R1A2009131) through NRF. Some portion of our computational work was done using the resources of the KISTI Supercomputing Center (KSC-2015-C3-023).

---

* Current address: LG Chem Research Park, Daejeon 34122, Korea

† Corresponding author. E-mail: gunnkim@sejong.ac.kr

‡ Corresponding author. E-mail: ykkwon@khu.ac.kr

[1] T. O. Cheng, Texas Hear. Inst. J. **34**, 392 (2007).

[2] S. H. Ferreira, S. Moncada, and J. R. Vane, Br. J. Pharmacol. **49**, 86 (1973).

[3] H. D. Lewis, J. W. Davis, D. G. Archibald, W. E. Steinke, T. C. Smitherman, J. E. Doherty, H. W. Schnaper, M. M. LeWinter, E. Linares, J. M. Pouget, et al., N. Engl. J. Med. **309**, 396 (1983).

[4] L. Chico, V. Crespi, L. Benedict, S. Louie, and M. Cohen, Phys. Rev. Lett. **76**, 971 (1996).

[5] S. J. S. Tans, A. R. M. A. Verschueren, and C. Dekker, Nature **393**, 49 (1998).

[6] Y.-K. Kwon, D. Tomanek, and S. Iijima, Phys. Rev. Lett. **82**, 1470 (1999).

[7] Y. Z, H. Postma, B. L, and D. C, Nature **402**, 273 (1999).

[8] S. Sanvito, Y.-K. Kwon, D. Tománek, and C. J. Lambert, Phys. Rev. Lett. **84**, 1974 (1999).

[9] S. Berber, Y.-K. Kwon, and D. Tomanek, Phys. Rev. Lett. **84**, 4613 (2000).

[10] C. Zhou, J. Kong, E. Yenilmez, and H. Dai, Science (80-.). **290**, 1552 (2000).

[11] J. Lee, H. Kim, S.-J. Kahng, G. Kim, Y.-W. Son, J. Ihm, H. Kato, Z. W. Wang, T. Okazaki, H. Shinohara, et al., Nature **415**, 1005 (2002).

[12] G. Kim, S. B. Lee, T. S. Kim, and J. Ihm, Phys. Rev. B **71** (2005).

[13] J.-C. Charlier, X. Blase, and S. Roche, Rev. Mod. Phys. **79**, 677 (2007).

[14] W. I. Choi, J. Ihm, and G. Kim, Appl. Phys. Lett. **92**, 1 (2008).

[15] R. Q. Long and R. T. Yang, Ind. Eng. Chem. Res. **40**, 4288 (2001).

[16] M. Cinke, J. Li, B. Chen, A. Cassell, L. Delzeit, J. Han, and M. Meyyappan, Chem. Phys. Lett. **365**, 69 (2002).

[17] Y. F. Yin, T. Mays, and B. McEnaney, Langmuir **16**, 10521 (2000).

[18] A. C. Dillon, K. M. Jones, T. A. Bekkedahl, C. H. Kiang, D. S. Bethune, and M. J. Heben, Nature **386**, 377 (1997).

[19] A. Chambers, C. Park, R. T. K. Baker, and N. M. Rodriguez, J. Phys. Chem. B **102**, 4253 (1998).

[20] X. Peng, Y. Li, Z. Luan, Z. Di, H. Wang, B. Tian, and Z. Jia, Chem. Phys. Lett. **376**, 154 (2003).

[21] S. B. Fagan, A. G. Souza Filho, J. O. G. Lima, J. Mendes Filho, O. P. Ferreira, I. O. Mazali, O. L. Alves, and M. S. Dresselhaus, Nano Lett. **4**, 1285 (2004).

[22] S. B. Fagan, E. C. Girão, J. M. Filho, and A. G. S. Filho, Int. J. Quantum Chem. **106**, 2558 (2006).

[23] F. Tournus, S. Latil, M. Heggie, and J.-C. Charlier, Phys. Rev. B **72**, 075431 (2005).

[24] J. Kong, Science **287**, 622 (2000).

[25] H. J. Song, Y. Lee, T. Jiang, A. G. Kussow, M. Lee, S. Hong, Y.-K. Kwon, and H. C. Choi, J. Phys. Chem. C **112**, 629 (2008).

[26] P. G. Collins, Science **287**, 1801 (2000).

[27] K. Bradley, J. C. P. Gabriel, A. Star, and G. Grüner, Appl. Phys. Lett. **83**, 3821 (2003).

[28] M.-F. Yu, B. S. Files, S. Arepalli, and R. S. Ruoff, Phys. Rev. Lett. **84**, 5552 (2000).

[29] D. P. Burt, N. R. Wilson, J. M. R. Weaver, P. S. Dobson, and J. V. Macpherson, Nano Lett. **5**, 639 (2005).

[30] Y. Zhang, A. Thomas, M. Antonietti, and X. Wang, J. Am. Chem. Soc. **131**, 50 (2009).

[31] D. Li, X. Chu, S.-C. Cheng, X.-W. Lin, V. P. Dravid, Y.-W. Chung, M.-S. Wong, and W. D. Sproul, Appl. Phys. Lett. **67**, 203 (1995).

[32] B. L. M. Zambov, C. Popov, N. Abedinov, M. F. Plass, W. Kulisch, T. Gotszalk, P. Grabiec, I. W. Rangelow, and R. Kassing, Adv. Mater. **12**, 656 (2000).

[33] C. Cao, F. Huang, C. Cao, J. Li, and H. Zhu, Chem. Mater. **16**, 5213 (2004).

[34] Q. Guo, Y. Xie, X. Wang, S. Zhang, T. Hou, and S. Lv, Chem. Commun. **1**, 26 (2004).

[35] J. Li, C. Cao, and H. Zhu, Nanotechnology **18**, 115605 (2007).

[36] H. Pan, Y.-W. Zhang, V. B. Shenoy, and H. Gao, Nanoscale Res. Lett. **6**, 97 (2011).

[37] P. Hohenberg and W. Kohn, Phys. Rev. B **136**, B864 (1964).

[38] W. Kohn and L. J. Sham, Phys. Rev. **140** (1965).

[39] G. Kresse and J. Hafner, Phys. Rev. B **47**, 558 (1993).

[40] G. Kresse, Phys. Rev. B **54**, 11169 (1996).

[41] J. Perdew, K. Burke, and M. Ernzerhof, Phys. Rev. Lett. **77**, 3865 (1996).

[42] S. Grimme, J. Comput. Chem. **27**, 1787 (2006).

[43] H. J. Monkhorst and J. D. Pack, Phys. Rev. B **13**, 5188 (1976).